

5-18-2021

From Biological into Electronic Vision: The Solution of Edge Detection Problem.

Yehia Enab

Assistant Professor of Control and Computer Department, Faculty of Engineering, Mansoura University, Mansoura, Egypt.

Follow this and additional works at: <https://mej.researchcommons.org/home>

Recommended Citation

Enab, Yehia (2021) "From Biological into Electronic Vision: The Solution of Edge Detection Problem.," *Mansoura Engineering Journal*: Vol. 15 : Iss. 1 , Article 8.
Available at: <https://doi.org/10.21608/bfemu.2021.170556>

This Original Study is brought to you for free and open access by Mansoura Engineering Journal. It has been accepted for inclusion in Mansoura Engineering Journal by an authorized editor of Mansoura Engineering Journal. For more information, please contact mej@mans.edu.eg.

**FROM BIOLOGICAL INTO ELECTRONIC VISION: THE SOLUTION OF
EDGE DETECTION PROBLEM**

BY

Dr. Yehia M. Enab
Lecturer in Control and Computer Department,
Faculty of Engineering
El-Mansoura University, El-Mansoura, EGYPT.

من الرؤية البيولوجية الى الرؤية الالكترونية :
هل مسألة استكشاف حواف الصورة

KEYWORDS:

Artificial intelligence, Neural networks, Hardware machine vision, Biomedical engineering,

ملخص

بعد هذا البحث اسهاما يضاف الى المحاولات المديشة التي تهدف الى عبور الفجوة بين التفسير البيولوجي و التفسير الرياضي للرؤية لدى عيون البشر. و اعتمد الباحث في ذلك على تفسير وناقش بعض الخلايا العصبية في شبكية العين على انها عمليات رياضية كالجمع و الطرح الجبري و هكذا التفاضل، و تحدد الاضافة الجديدة لهذا البحث في تصميم دائرة الالكترونية متعاملة تستخدم مبدأ المعالجة المتوازية للصورة لاستكشاف الحواف المطلوبة. و تتكون الدائرة من عناصر مظهر العمليات لمعالجة العمليات الرياضية و كذلك شبكة من المداومات الشبكية لمعالجة الأوزان المطلوبة التي تمثلها "المتاب" الشعيرات العصبية التي تربط بين الخلايا العصبية الفعلية. و هذه الدائرة تحاكي الطبقات الثلاثة الاولى من شبكية العين و هي "الصبغيات" و "الاقبية" و "القشرية"، و تم تحليل هذه الدائرة الالكترونية رياضيا لاثبات ان خرج هذه الدائرة يتقارب الى الحواف الفعلية للصورة. و يعتبر هذا البحث خطوة على طريق تصميم و انتاج انواع جديدة من الدوائر المتعاملة و التي تجعل الرؤية الالية و التما مصري و سهل مما يفتح آفاق واسعة لانتاج اجيال من الروبوتات الذكية.

ABSTRACT

This paper introduces an understanding of the role of certain types of neural cells in the vertebrate retina as a process for edge detection and localization. A design of an electronic neural edge detector is proposed and analyzed. Our hope is that this and similar efforts will eventually lead to the formation of engineering principles that will assist developments in the science and technology of the hardware electronic vision and machine perception. The proposed approach makes use of the biological findings established in the medical literatures associated with early visual processing in vertebrate retina. The use of neural networks is the optimal choice for the hardware implementation of the edge detector. The reason is that the concept of parallel processing is satisfied. This is similar to the role played by the physical neurons in vertebrate retina while processing the images. A computer simulation is used to test the performance of this approach.

(1) INTRODUCTION

Edge detection and localization is a well-known problem in machine vision. Edges are curves in the image where rapid changes occur in gray level or in the spatial derivatives of gray level. Edges in the images often result from "occluding contours" of the three-dimensional (3D) objects. These contours represent physical events which are very important to be detected by a useful vision system. Edges may also arise from discontinuities in surface orientation and reflectance properties.

Edge detection and localization is important for two reasons. First, it represents a "compact description" of the input image such that it is possible and easy to reconstruct the original signal from the representation. Second, the edge representation is a "meaningful" one, hence, it relates the raw input data (viewer-centered) to the physical events that cause it, in particular the objects being observed (object-centered). In fact, edge detection and localization is one of the initial tasks to be performed by the visual system as an early processing of the input image.

Many efforts have been done to understand the biological solution of the vision problem. Many researchers have been studied the vertebrate retina and the brain as a system performing a visual information processing. The retina codes the image into neural impulses that are eventually transmitted through the optic nerve to be analyzed by the brain which performs the perception and recognition tasks.

This paper introduces an understanding of the role of certain types of neural cells in the retina as a process for edge detection and localization. A design of neural edge detector is proposed and analyzed. Our hope is that this and similar efforts will eventually lead to the formation of engineering principles that will assist developments in the science and technology of the hardware electronic vision and machine perception. With this objective in mind, we have made conscious allowances in mapping the full complexity of the retinal organization onto a relatively simple network of causal relationships, which captures the important functional characteristics of the system.

(2) ORGANIZATION OF THE PAPER

The paper begins by reviewing the major approaches taken by previous researchers to accomplish edge detection, localization, and estimation. Then few of anatomical and physiological aspects of the neural structure for vertebrate retina are pointed out. After that, a review for some mathematical aspects of edge detection is introduced. This includes the ill-posed nature of the problem and the conditions under which edge detection can be transformed into a well-posed problem. In a later section the design of one dimensional (1D) edge detector is introduced. The analysis of the stability and convergence of the system response are investigated. The results of the computer simulation experiments used to test the stability and convergence of the system are discussed. Finally the paper ends with the conclusions and suggestions for further research.

(3) LITERATURE REVIEW

Edge detection has been one of the most active fields in machine vision. The use of convolutional edge-enhancement operator is used in the classic paper by Roberts [1]. This paper showed how to extract edges from the high quality photographs of polyhedral objects digitized on a converted drum plotter. Binford [2] realized that a large image area was needed to provide sufficient evidence for an edge in a noisy image.

There are many algorithms for detecting and locating edges using non-convolutional approaches. Duda & Hart [3] considered use of the "Hough transform", a mapping into the parameter space of the line sought after. Hueckel [4] developed a least-squares fitting scheme based on expansion of the brightness function in a region in terms of orthogonal functions. Haralick [5] proposed the use of a piecewise linear approximation of the brightness surface. Rosenfeld & Thurston [25] may have been the first to propose working on an image simultaneously at several levels of resolution. A very different approach to edge detection is based on stochastic models of the image is found in [26].

The "Laplacian" and various discrete approximation had been proposed for edge detection [6]. Modestino & Fries [7] obtained an optimal estimate of the Laplacian over a large support area. The "Gaussians" had been used in edge detection by Macleod [8]. A new theory of edge detection based on finding the "zero-crossings" of the output of an even-derivative operator applied to the image is described by Marr & Hildreth [9]. They took the Laplacian operator and combined it with the Gaussian smoothing filter to produce a rotationally symmetric edge operator.

Recently there has been more concern about the accuracy and sensitivity to noise of these edge-enhancement operators, see Hartley [10]. This is still an active area of research.

(4) BIOLOGICAL BACKGROUND

The processing of visual information in vertebrates begins with the absorption of photons of an incoming light by the photopigment molecule of the membranes at the specialized external segments of the retina. The retina in all vertebrates is constructed with five different types of cells: receptor cells (rods or cones), horizontal cells, bipolar cells, amacrine cells, and ganglion cells, which form a functional unit in which the processing of visual information begins. Since Cajal [11] originally classified vertebrate retinal neurons near the turn of the century, much work has been devoted to the characterization of individual cells and their functional role in the spatiotemporal organization of the retina. The intracellular microelectrode recordings have shown that the electrical activities of the first three cells (receptor, horizontal and bipolar) can be characterized as hyperpolarization or depolarization, which is increasing or decreasing the neuron membrane potential by either chemical or physical means [12,13,14]. The amacrine and ganglion cells give spike activity i.e., an on-off response [11].

In the retinal processing of light information, the very large range of light intensities of the outside world is compressed into a narrower range which can be handled

satisfactorily by the fibers of the optic nerve. The neurally coded visual message collected in the ganglion cells is transmitted by the optic nerve fibers to the thalamocortical cells located in the lateral geniculate nucleus and in the visual cortex where the higher visual processing occurs [15]. This processing includes the matching between the left and right images of the two eyes to sense the depth of the three-dimensional objects.

The main characteristics of the receptor, horizontal, and bipolar neurons in the vertebrate primary visual system is briefly outlined. The connections among the three types of cells are also described. The neural edge detector studied in the present work is constructed using electronic components, which simulate the functions of these cells.

1) Receptor Cells [15,16]

The first stage of vision is the physical interaction between light focused on the retina and the visual pigment in retinal cells. The human retina is composed of over 100 million light-sensitive cells. A small proportion of them near the center (about 6 million) are specialized to respond to light from one of three wavelengths, and these three sorts of cells- the so-called "cones"- are maximally sensitive to red, green, and blue respectively. The full range of perceived colors is based purely on these inputs. The remaining cells in the retina - the so-called "rods"- are less specialized, responding to light over a wide range of frequencies.

These cells are located in the outermost part of the retina. The electrical response of a receptor cell is proportional to the number of photons absorbed by the photopigment molecules of the cell membranes. The receptive field of a photoreceptor is very small and probably only as large as the receptor itself. The receptive field of a single visual neuron is defined as that region of the retina or visual field which, when presented with a photic stimulus, will lead to a change in the neural activity of the cell. This means that in general receptors do not make lateral connections with other receptors.

2) Horizontal Cells [17,18]

These cells are horizontally located just below the receptor cells in the retina and receive inputs from receptor cells via chemical synapses. The horizontal cell essentially acts as a low-pass filter. It performs an integrative function, summing responses of individual receptors to generate effectively a low-frequency offset potential for the bipolar cell. A positive feedback mechanism exists between receptors and horizontal cells. The horizontal cells are tightly packed to form a layer and there exist electrical synapses among adjacent cells within the layer. When a horizontal cell is depolarized, this depolarization propagates laterally and sums with the adjacent cell potential essentially performing an integrative function.

3) Bipolar Cells [19,20]

The bipolar cell, located in the inner nuclear layer, receives input from both the horizontal and receptor cells. Functional and morphological identification techniques have shown that both inputs are found on each bipolar cell, suggesting that these cells may function as common mode rejecting devices. The

cell subtracts the integrative low-frequency potential of the horizontal cell from the local response received directly from the receptors.

**(5) MATHEMATICAL ASPECTS OF ONE-DIMENSIONAL
EDGE DETECTION PROBLEM**

In a gray level image, an edge point is a point where intensity change is taking place. A simple model for edges will be used, namely a step edge. Let the i^{th} step edge at location x_1 with step size S_1 is denoted by $I_1(x)$:

$$I_1(x) = S_1 u(x - x_1) \quad (5.1)$$

where $u(x)$ is the unit step function. The waveform signal can be well approximated by the function $I(x)$ which is the sum of a edges:

$$\begin{aligned} I(x) &= \sum_{i=1}^N I_i(x) \\ &= \sum_{i=1}^N S_i u(x - x_i) \end{aligned} \quad (5.2)$$

where N is the number of pixels in the digital form of $I(x)$ (see Fig. 1). Edges can be classified into two types, one with small intensity S_1 and the other with sharp intensity. Edge detection problem can be formulated as: given a certain raw image $\{I(x_i), i=1, \dots, N\}$, it is required to detect the sharp changes S_1 's and their locations x_i 's in this image. Edges with small intensities are neglected, hence they do not represent physical events, instead they occur due to noise in lightening or sensing processes. The small intensity edges are usually cancelled by the averaging process.

It has been suggested [21] that edge detection is essentially a problem of numerical differentiation. Because differentiation amplifies high-frequency components, then after differentiation high frequencies of the noise will be enhanced and we lose stability or continuity from the initial data. In other words, the problem is ill-posed in the classical sense of Hadamard [22]. A well-posed problem is one with a solution that is unique and depends continuously on the data. A problem that fails either of these two criteria is called ill-posed. The discretization of an ill-posed problem often leads to an ill-conditioned system of equations - i.e., a system in which small errors in the data can lead to large errors in the solution. Differentiation, however, is a mildly ill-posed problem, which can be transformed into a well-posed problem by many methods [22]. A convenient way is to convolve the signal with Gaussian function $g(x)$. In vision literature, there are several descriptions of the analytic form of the Gaussian distribution, which differ only in an overall multiplicative constant that does not change the shape of the distribution. We adopt the following form

$$g(x) = \text{Exp.}[-x^2/2\sigma^2] \quad (5.3)$$

where σ is the variance. The Gaussian function is a low pass filter and it has a symmetrical shape as shown in Fig. 2.a. The noise free image $I_f(x)$ is given as:

$$I_f(x) = g(x) * I(x) \quad (5.4)$$

(* represents the convolution operation)

This image is used instead of the initial raw data $I(x)$ to make the edge detection problem as a well-posed one. In fact, there is a general agreement on the usefulness of filtering images before locating edges, but it is not obvious how to locate edges after filtration. There are two approaches, which although related, can give rather different results:

1) Extrema scheme:

Because edges are sharp changes in the gray level profile, they can be detected at the extrema of the convolution of the approximating signal $I(x)$ and of the first derivative of a Gaussian filter, i. e.,

$$H(x) = dg(x)/dx * I(x) \quad (5.5)$$

the step size S_j is the amount of the extrema and its position is the corresponding edge location x_j . The first derivative of a Gaussian $D(x)$ is determined from Eq. 5.3 as

$$D(x) = dg(x)/dx = (-x/\sigma^2) \text{Exp.}[-x^2/2\sigma^2] \quad (5.6)$$

This distribution is shown graphically in Fig. 2.b. A corresponding numerical mask used in the convolution process can be derived. The output of the convolution of the train of edges $I(x)$ (Eq. 5.2) with this filter is

$$\begin{aligned} H(x) &= D(x) * I(x) \\ &= \int_{-b}^{\infty} \left(\frac{-(x-\tau)}{\sigma^2} \text{Exp.}[-(x-\tau)^2/2\sigma^2] \right) \sum_{i=1}^N S_i u(\tau-x_i) d\tau \\ &= \sum_{i=1}^N S_i \int_{-b}^{\infty} \left(\frac{-(x-\tau)}{\sigma^2} \text{Exp.}[-(x-\tau)^2/2\sigma^2] \right) u(\tau-x_i) d\tau \\ &= \sum_{i=1}^N S_i \int_{x_i}^{\infty} d[\text{Exp.}-(x-\tau)^2/2\sigma^2] \\ &= -\sum_{i=1}^N S_i [\text{Exp.}-(x-\tau)^2/2\sigma^2]_{x_i}^{\infty} \\ &= \sum_{i=1}^N S_i \text{Exp.}[-(x-x_i)^2/2\sigma^2] \end{aligned} \quad (5.7)$$

It has been shown that edges detected as extrema of the gradient is a good description of the image [24].

ii) Zero-Crossings scheme

The zero-crossing is defined as a point where a function's

value changes its sign. If $I_f(x)$ is the filtered image, we can identify edges as zero-crossings of the convolution of the approximating signal and of a Laplacian over Gaussian LoG filter i. e.,

$$F(x) = d^2g(x)/dx^2 * I(x) \quad (5.8)$$

The second derivative of a Gaussian mask (defined in eq.5.3) is given as

$$L(x) = -(1/\sigma^2) [1-x^2/\sigma^2] \text{Exp.}[-x^2/2\sigma^2] \quad (5.9)$$

This mask is known as Laplacian of Gaussian (LoG) filter (see Fig. 2.c). Therefore the convolution of the approximating signal $I(x)$ and a LoG filter is

$$F(x) = L(x) * I(x) \quad (5.10)$$

In a similar manner as in Eq. (5.7) the following equation can be proved

$$F(x) = 1/\sigma^2 \sum_{i=1}^N S_j(x-x_i) \text{Exp.}[-(x-x_i)^2/2\sigma^2] \quad (5.11)$$

The edge is located at the zero crossing x_1 , the peak and valley are at a distance of σ on either side of x_1 , and their amplitudes are proportional to S_1 , the size of the step.

In fact, the application of a first-derivative operator must be followed by a search for peak values. A means of suppressing large values near the local maxima is also required. Partly for this reason, second-derivative operators became more popular, since the edge is located where their output is a zero crossing.

(6) ONE DIMENSIONAL NEURAL EDGE DETECTOR DESIGN

1) Receptor Layer

The receptor layer is modeled using an array of photodiodes. Each cell converts the amount of light captured by it into a corresponding analog electrical signal (see Fig. 3). The spatial distance between each two successive neurons corresponds to the image resolution, any image details less than this resolution can not be identified. The photodiodes are isolated from one to another, i. e., no inter-connections exist between them. Let $I(x_1, t), I(x_2, t), \dots, I(x_N, t)$ represent the analog signals outputted from the different receptor cells at locations x_1, x_2, \dots, x_N and time instant t , where N is the number of photodiodes in the receptor layer. During the following analysis it will be assumed that these signals are constants with time. The output of the j^{th} receptor cell will be denoted as $I(x_j)$. This output is modeled using the equation (5.2) as

$$I(x_j) = \sum_{i=1}^N S_i u(x_j - x_i) \quad (6.1)$$

11) Horizontal Layer

This layer is designed to obtain the different step sizes

$\{S_j, j=1,2, \dots, N\}$ at the different receptor cells. The value of the convolution of the first derivative of the signal $I(x_j)$ with the Gaussian $G(x)$ centered at the receptor located at x_j can be derived from Eq. (5.7) as

$$\begin{aligned} H_j &= H(x_j) \\ &= \sum_{i=1}^N S_i \text{Exp.}[-(x_j - x_i)^2/2\sigma^2] \end{aligned} \quad (6.2)$$

The above equation can be written in the form ; $j=1,2, \dots, N$

$$H_j = \sum_{i=1}^N S_i v_{ji} \quad (6.3)$$

where

$$v_{ij} = \text{Exp.}[-(x_j - x_i)^2] \quad (6.4)$$

The weight $w_{ij} = 1$ if $(x_i = x_j)$ and is always less than unity for any other combination of i, j . Equation 6.3 represents one equation in N unknowns $S_i, i=1,2, \dots, N$. The left hand side of this equation H_j is determined directly from the raw data $I(x)$ as the product of the numerical mask D corresponding to Fig. 2.b centered at point x_i and the raw data. In matrix form, Eq. (6.3) can be written as

$$\underline{H} = \underline{W} \underline{S} \quad (6.5)$$

\underline{H} is $(N \times 1)$ column matrix containing the values of $H_j, j=1,2, \dots, N$
 \underline{S} is $(N \times 1)$ column matrix containing the values of $S_i, i=1,2, \dots, N$
 \underline{W}_{ij} is $(N \times N)$ matrix containing the values of w_{ij}

Note that \underline{W} is an extremely well behaved matrix, symmetric, positive definite, with 1's on the diagonal. The inversion of this matrix is quite straight forward, leading to a set of values for the step sizes. For all practical purposes, it can also be considered as a band matrix, since the decrease along both sides of the diagonal is exponential. A band matrix of "band width" $[\theta_1, \theta_2]$ is a matrix for which $w_{ij} = 0$ if $i-j > \theta_1$ or $j-i > \theta_2$.

Experimental results shows that the full matrix can be very well approximated by a band matrix with band width of 5 pixels, which says that no more than 3 edges interact at any given point. Due to the above properties the Gauss-seidel method [25] is used to find the solution of Eq. 6.5, hence it is suitable to be implemented in a hardware form using the neural networks. This occurs by rewriting equation (6.2) as:

$$S_j = -\sum_{\substack{i=1 \\ i \neq j}}^N S_i \text{Exp.}[-(x_j - x_i)^2/2\sigma^2] + H_j \quad (6.6)$$

$j=1,2, \dots, N$

or

$$S_j = -\sum_{\substack{i=1 \\ i \neq j}}^N S_i W_{ij} + H_j \quad (6.7)$$

The connection between the receptor layer cell and the horizontal layer cell is performed via a weighted synapse. We denote by W_{ij} the synaptic weight of the output of neuron A_j in the receptors layer and the neuron A_i in the horizontal layer (see Fig. 3). In other words, W_{ij} represents the increment of the postsynaptic potential of A_i in the horizontal layer when a pulse arrives from the output of A_j in the receptor layer. When the output of A_i is not connected to A_j , we put $W_{ij} = 0$. Due to the properties of the matrix W , the output of the horizontal layer converges despite the initial state of the output. The N^2 synaptic weights W_{ij} ($i, j = 1, 2, \dots, N, i \neq j$) constitute an $N \times N$ matrix C which we call the "connection matrix". It represents the interconnection of neurons in the net. It is important to note that $c_{ij} = -w_{ij}$ for $i \neq j$ and $c_{ij} = 0$ for $i = j$, i.e., the main diagonal contains zero elements. Physically, this means that no feedback occurs from a single neuron in the horizontal layer to itself.

iii) Bipolar layer

The bipolar layer is designed to obtain the locations of the different edges corresponding to sharp variations in S_j . The bipolar layer is composed of N cells, each cell is an operational amplifier functions as a comparator. This comparator obtains the difference of two Gaussians (DoG). The first Gaussian is derived from the original raw data (the output of the receptor layer). The second Gaussian is derived from the estimated extrema of the raw data (the output of the horizontal layer). The output of the comparator is a logical one (1) if and only if the two inputs are equal, in other words the difference of the two Gaussians is zero, else the output is zero. This means that the output of the bipolar layer is rhythmic response and the ones correspond to the desired edges of the image.

The first Gaussian is implemented through the use of suitable weights for the synapses connecting each cell in the bipolar layer with the different cells in the receptor layer. This weight is denoted by U_{ij} and can be determined from eq. (5.9) as

$$U_{ij} = \frac{-1}{\sigma^2} [1 - (x_i - x_j)^2 / \sigma^2] \text{Exp.} [-(x_i - x_j)^2 / 2\sigma^2] \quad (6.8)$$

$i, j = 1, 2, \dots, N$

This Gaussian is denoted as $L_1(x_j)$ which represents the LoG for the raw image determined at point x_j . This value is given as

$$L_1(x_j) = \sum_{i=1}^N U_{ij} I(x_i) \quad (6.9)$$

; $j=1,2,\dots,N$

The second Gaussian is implemented through the use of suitable weights for the synapses connecting each cell in the bipolar layer with the different cells in the horizontal layer. This weight is denoted by V_{ji} and can be determined from eq. (5.11) as

$$V_{ji} = 1/\sigma^2 (x_j - x_i) \text{Exp.}[-(x_j - x_i)^2/2\sigma^2] \quad (6.10)$$

$i, j = 1, 2, \dots, N$

This Gaussian is denoted as $L_2(x_j)$ which represents the LoG for the raw image determined at point x_j (see Fig. 3). This value is given as

$$L_2(x_j) = \sum_{i=1}^N V_{ji} S_i \quad (6.11)$$

It is useful now to indicate the difference between the technique used to localize the edge in this paper and the Difference of Gaussians (DoG) technique known in the literatures. The DoG technique locates the edge at the zero crossing of the Laplacian over Gaussian (LoG) of the original raw data using two Gaussians with different variance σ . In this paper, the edge is located at the zero crossing of two different LoG's with the same variance parameter σ . The first LoG is calculated directly from the original raw data and the other is calculated from the estimated step sizes derived from the original raw data.

It is important to mention here that the one-dimensional neural edge detector can be used to detect the edges in a two dimensional (2D) image. This occurs by scanning the 2D image row by row or column by column as shown in the next section. In fact, it will be better to develop a 2D edge detector to extract the edges directly from the 2D images. Such detector is under development at this time.

(7) EXPERIMENTAL RESULTS

In this section, some results of the use of the proposed electronic edge detector are presented.
Simulation of neural edge detector:

The one dimensional electronic edge detector is simulated via a software subroutine according to the design rules described previously. In this routine there are three arrays R, H, B. The number of cells in each array is chosen to be 256. The input to this routine is the array R containing the raw data representing the output of the receptor layer. These data are generated either from artificial images or real images as indicated in the experiments described later in this section. The array H contains the estimated step sizes at each pixel of the raw data. The output of the subroutine is the array B. It represents the output of the bipolar layer. Each element of this array has a binary value. It is a logical 1 at the corresponding edge location, otherwise it is

a logical 0.

A Gaussian mask with certain variance (σ) is used to evaluate the different synaptic weights connecting the neurons in the different layers. In the simulation subroutine there are three weighting arrays W, U, V, each is one dimensional. The W array contains the weights of the connection between the receptor and the horizontal layers, the U array contains the weights of the connection between the horizontal and the bipolar layers, and the V array contains the weights of the connection between the receptor and the bipolar layers. The length of these arrays is the same and depends on the chosen σ of the Gaussian distribution. As an example if σ is 5 pixels, it is found that the length of the weighting arrays should be 21.

The action of the different operational amplifiers to reach its steady-state response is simulated by an iterative process. In the simulation process, it was found that about 100 iterations (in some cases) are required to reach an acceptable estimation of the edge location when using an XT personal computer and FORTRAN language. In fact, this number of iterations does not mean anything when the neural edge detector is implemented in hardware. This is because, theoretically the neural network can reach its steady state in no time, hence there is no clock pulses to organize the serial operations. Physically some time is consumed by the neural network to reach its stable state. This time is limited by the settling time of the used operational amplifiers which is about 10^{-9} sec for the nominal amplifiers.

Example 1: Ideal step edge

The image used is 256x256 pixels in size, with gray level values between 0 and 255. The height of the step edge is 50; the gray level on either sides of the edge were 10 and 160 respectively. Fig. 4.a shows the ideal image, and Fig. 4.b shows one dimensional horizontal slice of it. The image described previously is generated via a software program and stored in a file to be accessed by the neural edge detector routine. The image is scanned row by row, the results are shown in Fig. 4.c.

Example 2: Ideal edge in noise

A zero mean independently identically distributed Gaussian noise was added to the above image. Fig. 5.a shows the noise corrupted step edge with a signal to noise ratio (SNR) of 0.25. Signal to noise ratio is defined as

$$SNR = (h/\sigma_n)^2$$

where h is the edge step height and σ_n is the standard deviation of the Gaussian noise. In the presence of noise, we must use larger filters in order to reduce the number of false edges. The synaptic weights are determined using a Gaussian function with $\sigma=7$ pixels. Fig. 5.b shows a slice of the noisy image. Fig. 5.c shows the reconstructed signal using the electronic edge detector. Fig. 5.d shows the total edge for the whole image.

Example 3: Real images

The responses of retinal cells and of an electronic camera comprise, in effect, a two-dimensional array of the intensity values at each point on the light-sensitive surfaces. These values

can be represented as numerals (the larger the numeral, the more intense the light). If we ignore colour, these numerals can be converted back into shades of grey and thus into a picture known as the "grey-level image". Fig. 6.1 shows a grey-level image which is a point-by-point representation of the intensity values of a scene (576x454) pixels [27]. Fig. 6.2 shows the intensity values for the part of Fig. 5.1 inside the rectangle on the right-hand side. It is two-dimensional array [31x31] elements. Actually the human retina yields an array with vastly more elements, This image is processed by the edge detector routine. The results are derived from first processing the image row-by-row, which is now a one-dimensional processing and we can apply our approach directly, then processing the image column-by-column, finally ORing the results from both directions. Fig. 6.3 shows the estimated edges for the studied part of the image.

Accuracy of edge localization:

The average error in edge localization (ρ) is estimated as

$$\rho = (1/M) \sum_{k=1}^M |R_a - R_e|$$

where,

R_a = actual edge point location

R_e = estimated edge point location M = number of all edge points

in the whole image.

It is important from the economical point of view to define the suitable variance σ of the Gaussian distribution used to determine the different synaptic weights. Physically these weights are implemented using electrical resistances. The number of these resistances should be reduced as much as possible in order to minimize the power loss and consequently the heating effect. Fig. 7 shows the variation of the average edge localization accuracy as a function of the variance σ for both ideal image used in example 1 and noise image used in example 2. As shown from this figure the accuracy increases as the variance σ increases. For the noise-free image the saturation of the curve occurs at $\sigma=5$ pixels, and for noisy image $\sigma=7$ is suitable.

(7) CONCLUSIONS AND FUTURE RESEARCH

There are two contributions for this work. The first is the use of the biological findings associated with early visual processing in vertebrate retina to solve quantitatively the edge detection problem which is one of the basic problems in machine vision field. This occurs through the interpretation of the results established in the medical literatures using the mathematical theory for edge detection problem developed independently in the computer vision community.

The second contribution of this work is the use of neural networks as the optimal choice for the hardware implementation of the electronic edge detector. The reason is that the concept of parallel processing is satisfied. This is similar to the role played by the physical neurons in vertebrate retina while

processing the images.

The paper also introduced a complete design for the proposed electronic neural edge detector. The magnitude and the sign of the step sizes are estimated as the output of the horizontal layer, and the edges themselves appears at the output of the bipolar layer. The author believes that the human brain can approximate and reconstruct the original image from these outputs. The results shows that the detector works very well not only on some ideal signals, but also on real image data. The system stability and convergence are satisfied through the proper choice of the synaptic weights connecting the different neurons.

A good extension of the one-dimensional neural edge detector (1DNED) proposed is the (2DNED), even though the solution might involve more complexity. Another extension for this work is the study of the other neurons in the human visual system in order to obtain a suitable interpretation for the human stereo vision. This helps in developing a hardware vision system which will be excellent for robots to explore the surrounding environment without direct contact.

There are limitations with the proposed system when the edge model does not fit. For example, in the case where a "sloped" edge is involved, such as a ramp, or when there is a slope difference on the two sides of a step, the proposed model is no longer appropriate and just tries to make the best interpretation with the ideal step edge model. The modification of the model to fit with the different types of edges is a good area for research.

REFERENCES

- 1) L. G. Roberts, "Machine Perception of three-dimensional solids," in Optical and Electro-Optical Information Processing, J. T. Tippett et al. (eds.), MIT Press, Cambridge, Massachusetts, 1965, pp. 159-197.
- 2) T. O. Binford, "Inferring surfaces from Images," Artificial Intelligence, vol. 17, nos. 1-3, August 1981, pp. 205-244,
- 3) R. O. Duda, & P. E. Hart, "Use of Hough transformation to detect lines and curves in pictures," Communications of the ACM, vol. 15, no. 1, January 1972, pp. 11-15.
- 4) M. Hueckel "A local vision operator which recognizes edges and lines," Journal of the ACM, vol. 20, no. 4, October 1973, pp. 634-647.
- 5) R. M. Haralick, "Digital step edges from zero crossing of second directional derivatives," IEEE Trans. on Pattern Analysis and Machine Intelligence, vol. 6, no. 1, January 1984, pp. 58-68.
- 6) B. K. P. Horn, "VISMEN: A bag of robotics formulae," MIT AI Laboratory Working Paper 34, December 1972. 7) J. W. Modestino, & R. W. Fries, "Edge detection in noisy images using recursive digital filtering," Computer Graphics and Image Processing, vol. 6, no. 5, October 1977, pp. 409-433. 8) I. D. G. Macleod, "A study in automatic photo-interpretation," Ph.D. Thesis, Dept. of Engineering Physics, Australian National Univ., Canberra, Australia, March 1970.
- 9) D. Marr, & E. Hildreth, "Theory of edge detection," Proc. of the Royal Society of London B, vol. 207, 1980, pp. 187-217.
- 10) R. Hartley, "A Gaussian-weighted multi-resolution edge

- detector," *Computer Vision, Graphics and Image Processing*, vol. 30, no. 1, April 1985, pp. 70-83.
- 11) S. R. Cajal, "La retine des vertebrales," *La Cellule*, vol. 9, 1883, pp. 17-257.
 - 12) D. A. Baylor, "Retinal specialization for the processing of small signals," in *Theoretical Approaches in Neurobiology*, E. Reichardt and T. Poggio, Eds. Cambridge, MA: MIT Press, 1981, pp. 18-27.
 - 13) A. L. Byzov and Y. A. Trifonov, "Ionic mechanisms underlying the nonlinearity of horizontal cell membrane," *Vision Res.*, vol. 21, 1981, pp. 1573-1578.
 - 14) E. V. Famiglietti, Jr., "Functional architecture of cone bipolar cells in mammalian retina," *Vision Res.*, vol. 21, 1981, pp. 1559-1563.
 - 15) P. Z. Marmarelis and K. I. Naka, "Nonlinear analysis and synthesis of receptive field responses in the catfish retina. II. One-input white noise analysis," *J. Neurophysiol.*, vol. 36, 1973, pp. 619-633.
 - 16) K. I. Naka, "Factors influencing the time course of S-potentials resulting from brief flashes," *J. Physiol.*, vol. 200, 1969, pp. 373-385.
 - 17) M. Piccolino, J. Neyton, and H. M. Gershenfeld, "Peripheral antagonism in the small field L-horizontal cells (L2-HC) of turtle retina," *Vision Res.*, vol. 21, 1981, pp. 1579-1580.
 - 18) M. N. Oguztoreli, "Modeling and simulation of vertebrate primary visual system: Basic Network," *IEEE Transactions on Systems, Man, and Cybernetics*, vol. SMC-13, no. 5, September/October 1983, pp. 766-781.
 - 19) K. I. Naka, P. Z. Marmarelis, and R. Y. Chan, "Morphological and functional identification of catfish retinal neuron. III. Functional identification," *J. Neurophysiol.*, vol. 38, 1975, pp. 92-131.
 - 20) J. C. Curlander and V. Z. Marmarelis, "Processing of visual information in the distal neurons of the vertebrate retina," *IEEE Transactions on Systems, Man, and Cybernetics*, vol. SMC-13, no. 5, September/October 1983, pp. 934-943.
 - 21) M. Bertero, T. Poggio, and V. Torre, "Ill-posed problems in early vision," *Proc. IEEE*, 1988.
 - 22) E. DE Michell, B. Caprile, P. Ottonello, and V. Torre, "Localization and noise in edge detection," *IEEE Transactions on Pattern Analysis and Machine Intelligence*, Vol. PAMI-11, No. 10, October 1989.
 - 23) V. Torre and T. Poggio, "On edge detection," *IEEE Trans. on Pattern Anal. Machine Intell.* Vol. PAMI-8, Feb. 1986, pp. 147-168.
 - 24) J. F. Canny, "Finding Edge and Lines," M. I. T., Cambridge, Tech. Rep. 720, 1983.
 - 25) A. Rosenfeld, & M. Thurston, "Edge and curve detection for visual scene analysis," *IEEE Trans. on Computers*, vol. 20, no. 5, May 1971, pp. 562-569.
 - 26) D. B. Cooper, F. Sung, & P. S. Schencker, "Towards a theory of multiple-window algorithms for fast adaptive boundary finding in computer vision," Internal Report ENG-PRMI 80-3, Division of Engineering, Brown Univ., Providence, Rhode Island, July 1980.
 - 27) T Poggio, "Vision by man and machine," *Scientific American*, April 1984, p. 70.

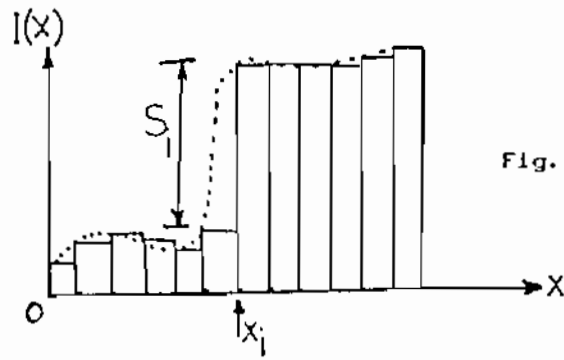


Fig. 1 Signal modeling

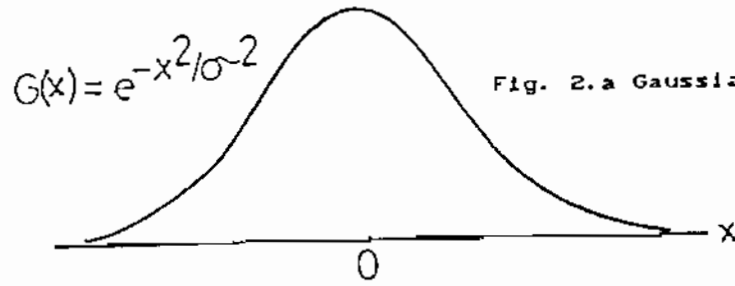


Fig. 2.a Gaussian distribution

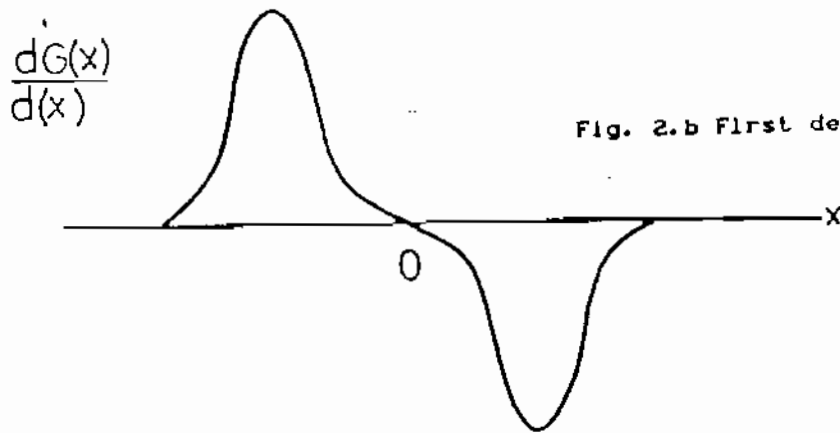


Fig. 2.b First derivative

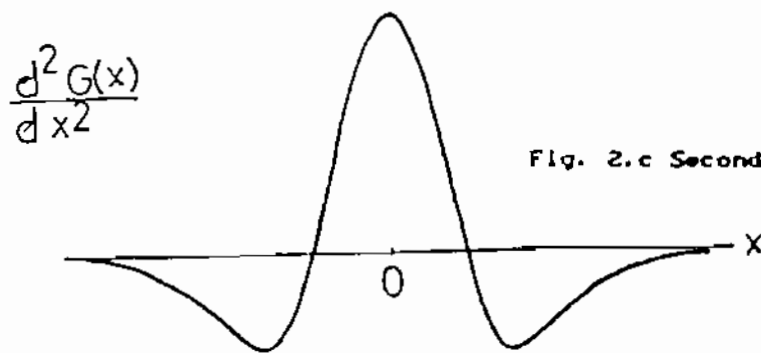


Fig. 2.c Second derivative

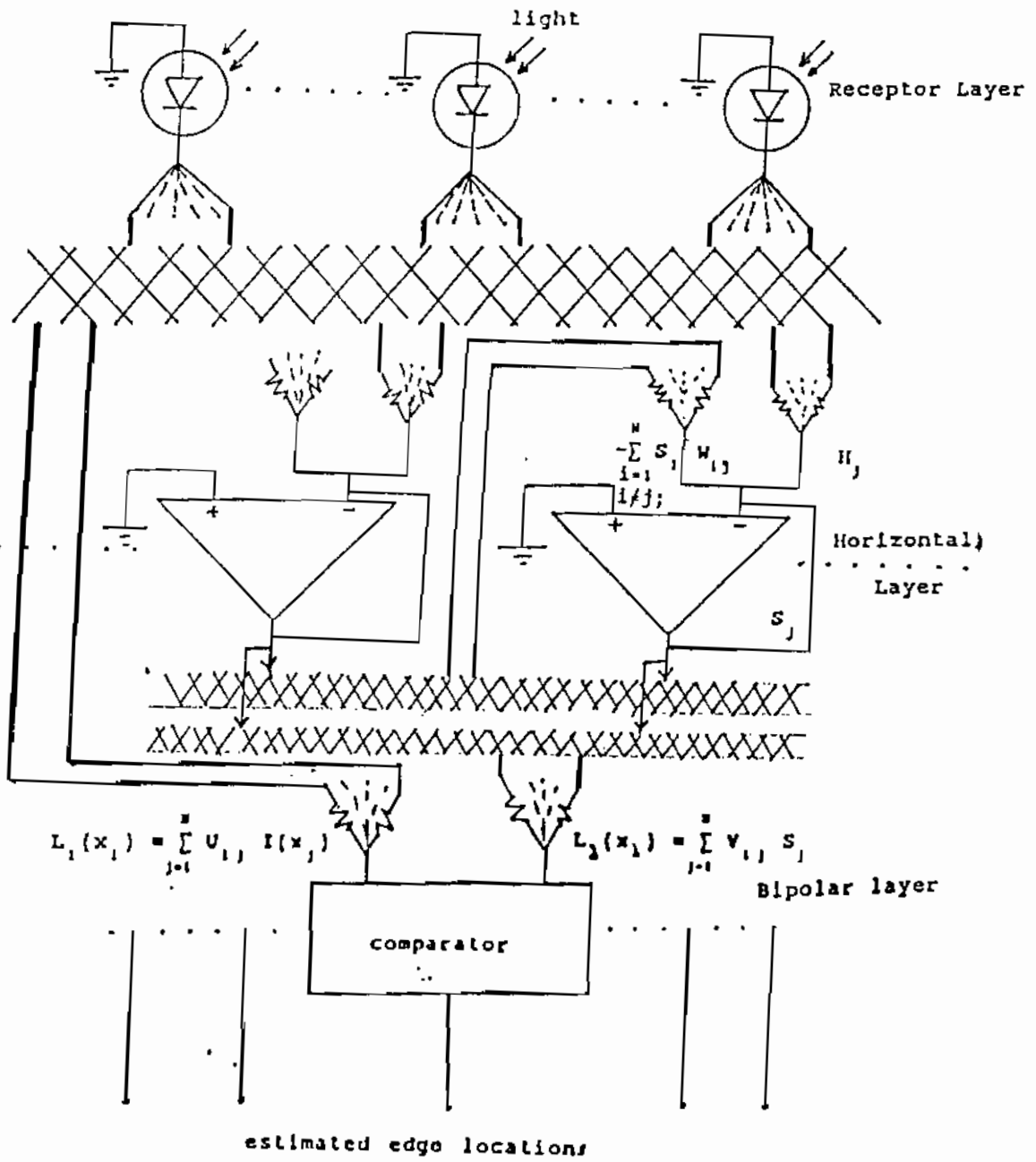


Fig. 3 Electronic neural edge detector

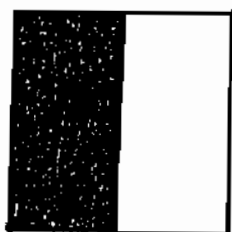


Fig. 4.a Ideal step edge

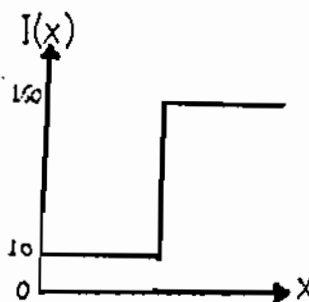


Fig. 4.b Horizontal slice

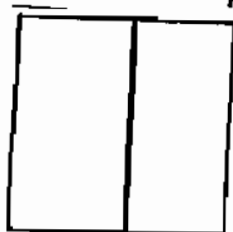


Fig. 4.c Estimated edge



Fig. 5.a Noisy image

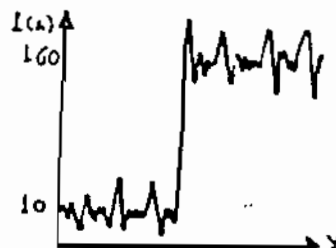


Fig. 5.b Horizontal slice

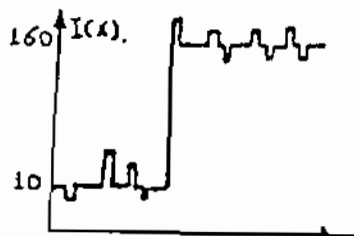


Fig. 5.c Reconstructed slice

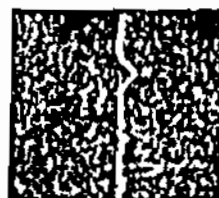


Fig. 5.d Estimated edge

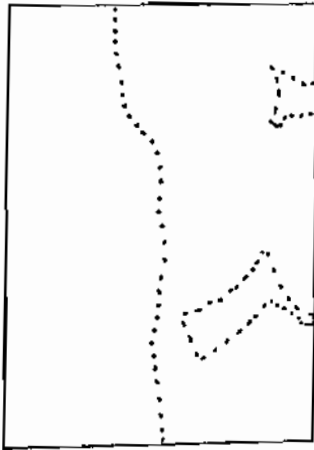


Fig. 6.3 Estimated edge for the real image inside the rectangle



Fig. 6.1 A grey-level image

| | | | | | | | | | | | | | | | | |
|-----|-----|-----|-----|-----|-----|-----|-----|-----|-----|-----|-----|-----|-----|-----|-----|-----|
| 225 | 221 | 216 | 210 | 219 | 214 | 207 | 218 | 219 | 220 | 207 | 155 | 136 | 135 | 130 | 131 | 128 |
| 213 | 206 | 213 | 223 | 208 | 217 | 223 | 221 | 223 | 216 | 195 | 156 | 141 | 130 | 128 | 138 | 123 |
| 206 | 217 | 210 | 216 | 224 | 223 | 228 | 230 | 234 | 216 | 207 | 157 | 136 | 137 | 137 | 130 | 128 |
| 211 | 213 | 221 | 223 | 220 | 222 | 237 | 216 | 219 | 220 | 178 | 149 | 137 | 132 | 128 | 138 | 121 |
| 216 | 210 | 231 | 227 | 224 | 238 | 231 | 218 | 195 | 227 | 161 | 141 | 131 | 133 | 131 | 124 | 122 |
| 223 | 229 | 216 | 230 | 218 | 214 | 213 | 208 | 198 | 224 | 161 | 140 | 133 | 127 | 133 | 122 | 133 |
| 230 | 219 | 224 | 228 | 219 | 215 | 215 | 208 | 206 | 221 | 159 | 143 | 133 | 121 | 128 | 127 | 127 |
| 221 | 215 | 211 | 214 | 220 | 218 | 211 | 212 | 210 | 204 | 148 | 141 | 131 | 130 | 128 | 129 | 118 |
| 214 | 211 | 211 | 216 | 214 | 220 | 229 | 216 | 223 | 208 | 143 | 141 | 141 | 134 | 121 | 132 | 125 |
| 211 | 208 | 223 | 211 | 216 | 216 | 211 | 210 | 211 | 198 | 153 | 141 | 136 | 125 | 131 | 125 | 130 |
| 205 | 224 | 214 | 214 | 217 | 221 | 232 | 211 | 210 | 211 | 148 | 139 | 128 | 132 | 128 | 124 | 132 |
| 204 | 208 | 204 | 205 | 233 | 241 | 241 | 242 | 247 | 162 | 151 | 141 | 137 | 130 | 127 | 128 | 129 |
| 208 | 205 | 201 | 216 | 232 | 248 | 255 | 246 | 251 | 210 | 148 | 141 | 132 | 128 | 126 | 128 | 129 |
| 199 | 194 | 208 | 238 | 243 | 253 | 248 | 236 | 230 | 167 | 148 | 139 | 138 | 132 | 129 | 132 | 123 |
| 199 | 199 | 200 | 227 | 238 | 237 | 225 | 236 | 217 | 162 | 148 | 142 | 124 | 133 | 125 | 126 | 128 |
| 198 | 198 | 209 | 211 | 216 | 215 | 218 | 210 | 232 | 177 | 142 | 137 | 135 | 124 | 128 | 127 | 128 |
| 198 | 203 | 205 | 200 | 211 | 224 | 228 | 210 | 210 | 198 | 138 | 137 | 129 | 126 | 122 | 124 | 131 |
| 214 | 208 | 211 | 228 | 216 | 231 | 245 | 218 | 199 | 143 | 148 | 129 | 128 | 126 | 124 | 128 | 123 |
| 211 | 218 | 217 | 216 | 216 | 227 | 244 | 211 | 162 | 148 | 138 | 128 | 133 | 131 | 122 | 126 | 128 |
| 215 | 210 | 214 | 216 | 208 | 220 | 214 | 208 | 156 | 138 | 131 | 129 | 138 | 128 | 122 | 130 | 128 |
| 219 | 220 | 211 | 209 | 205 | 208 | 210 | 217 | 154 | 141 | 127 | 130 | 134 | 147 | 134 | 128 | 129 |
| 229 | 224 | 217 | 214 | 228 | 229 | 224 | 208 | 151 | 145 | 128 | 128 | 142 | 127 | 128 | 132 | 124 |
| 232 | 221 | 222 | 224 | 233 | 244 | 228 | 213 | 143 | 141 | 126 | 128 | 131 | 128 | 128 | 124 | 131 |
| 235 | 235 | 230 | 248 | 253 | 248 | 238 | 193 | 147 | 139 | 132 | 128 | 139 | 125 | 128 | 128 | 119 |
| 250 | 245 | 238 | 243 | 248 | 235 | 235 | 198 | 138 | 138 | 134 | 125 | 126 | 138 | 128 | 127 | 132 |
| 210 | 238 | 233 | 232 | 235 | 255 | 246 | 164 | 154 | 141 | 128 | 127 | 126 | 134 | 125 | 128 | 128 |
| 241 | 242 | 225 | 219 | 225 | 235 | 163 | 139 | 141 | 128 | 130 | 128 | 137 | 128 | 126 | 130 | 130 |
| 234 | 218 | 221 | 217 | 211 | 252 | 248 | 164 | 138 | 132 | 130 | 125 | 128 | 127 | 121 | 132 | 132 |
| 231 | 221 | 214 | 214 | 218 | 225 | 238 | 171 | 145 | 145 | 124 | 134 | 131 | 124 | 121 | 128 | 131 |
| 238 | 212 | 214 | 214 | 213 | 208 | 218 | 168 | 134 | 138 | 138 | 134 | 128 | 127 | 127 | 124 | 122 |
| 238 | 212 | 215 | 215 | 208 | 215 | 227 | 161 | 128 | 141 | 128 | 128 | 131 | 128 | 125 | 128 | 127 |

Fig. 6.2 The intensity values for the part of Fig. 6.1 inside the rectangle on the right-hand side.

Localization error (pixels)

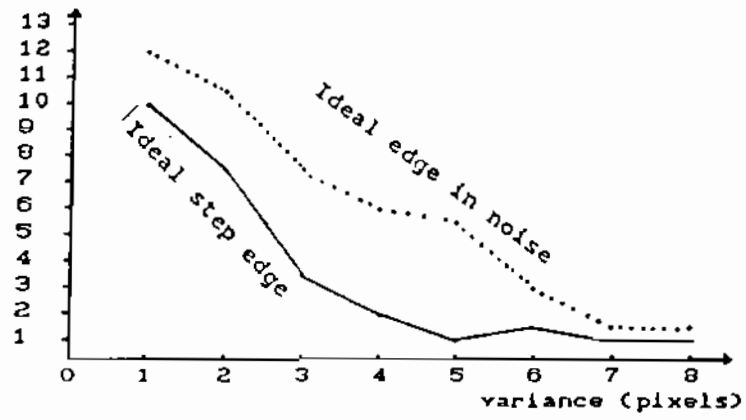


Fig. 7 Error in edge localization